

# Transcutaneous ultrasound-mediated gene delivery into canine livers achieves therapeutic levels of factor VIII expression

Megan A. Manson,<sup>1,\*</sup> Feng Zhang,<sup>2,\*</sup> Alexander Novokhodko,<sup>1</sup> Chun-Yu Chen,<sup>1</sup> Maura Parker,<sup>3</sup> Keith R. Loeb,<sup>3,4</sup> Masaki Kajimoto,<sup>1</sup> Carley Campbell,<sup>1</sup> Rainer F. Storb,<sup>3,5</sup> and Carol H. Miao<sup>1,6</sup>

<sup>1</sup>Center for Immunity and Immunotherapies, Seattle Children's Research Institute, Seattle, WA; <sup>2</sup>Department of Radiology, University of Washington, Seattle, WA; <sup>3</sup>Clinical Research Division, Fred Hutchinson Cancer Research Center, Seattle, WA; and <sup>4</sup>Department of Pathology, <sup>5</sup>Department of Medicine, and <sup>6</sup>Department of Pediatrics, University of Washington, Seattle, WA

## Key Points

- Nonviral UMGD can achieve therapeutic levels of FVIII gene expression in a large animal model.
- UMGD targeting liver is safe without evidence of any lasting damage.

A safe, effective, and inclusive gene therapy will significantly benefit a large population of patients with hemophilia. We used a minimally invasive transcutaneous ultrasound-mediated gene delivery (UMGD) strategy combined with microbubbles (MBs) to enhance gene transfer into 4 canine livers. A mixture of high-expressing, liver-specific human factor VIII (hFVIII) plasmid and MBs was injected into the hepatic vein via balloon catheter under fluoroscopy guidance with simultaneous transcutaneous UMGD treatment targeting a specific liver lobe. Therapeutic levels of hFVIII expression were achieved in all 4 dogs, and hFVIII levels were maintained at a detectable level in 3 dogs throughout the 60-day experimental period. Plasmid copy numbers correlated with hFVIII antigen levels, and plasmid-derived messenger RNA (mRNA) was detected in treated livers. Liver transaminase levels and histology analysis indicated minimal liver damage and a rapid recovery after treatment. These results indicate that liver-targeted transcutaneous UMGD is promising as a clinically feasible therapy for hemophilia A and other diseases.

## Introduction

In previous studies, we established the feasibility of using transcutaneous ultrasound-mediated gene delivery (UMGD) to deliver reporter luciferase plasmids to hepatocytes.<sup>1-3</sup> We aim to optimize this technique to treat genetic diseases that affect liver-specific proteins, particularly targeting hemophilia A, an X-linked recessive disorder that results in the loss of functional factor VIII (FVIII) protein and occurs in ~1 in every 5000 live male births.<sup>4</sup> FVIII is an important positive feedback regulator in the blood coagulation cascade, the loss of which results in a clotting deficiency ranging from mild to severe. FVIII protein replacement therapy,<sup>5-7</sup> which is the typical standard of care, requires repeated dosing 2 to 3 times per week, and it is highly burdensome for patients.<sup>4,8,9</sup> Significant advancements such as extended half-life FVIII and novel antibody treatment emicizumab have emerged in recent years<sup>7,10</sup>; however, both options still require frequent administration, and breakthrough bleeding is possible.<sup>11,12</sup> Therefore, gene therapy presents an attractive, more permanent solution for those with hemophilia A.

Recent studies, including those from our laboratory, have shown that UMGD is a safe and reliable method of gene delivery.<sup>1-3,13</sup> Compared with viral methods, UMGD has the benefit of reduced immunologic complications because it uses mechanical disturbance of cells instead of using viral vectors, which are known to elicit an immune response and are potentially toxic.<sup>14</sup> UMGD is most effectively

Submitted 25 August 2021; accepted 3 April 2022; prepublished online on *Blood Advances* First Edition 15 April 2022; final version published online 17 June 2022. DOI 10.1182/bloodadvances.2021006016.

\*M.A.M. and F.Z. contributed equally to this study.

Requests for data sharing may be submitted to Carol H. Miao (carol.miao@seattlechildrens.org).

The full-text version of this article contains a data supplement.

© 2022 by The American Society of Hematology. Licensed under Creative Commons Attribution-NonCommercial-NoDerivatives 4.0 International (CC BY-NC-ND 4.0), permitting only noncommercial, nonderivative use with attribution. All other rights reserved.

accomplished by sonoporation, which results from the cavitation of microbubbles (MBs). Upon exposure to ultrasound, MBs cavitate to create transient pores or disruption in vasculature and cellular and/or nuclear membranes.<sup>15-17</sup> The nonviral vector, naked plasmid DNA, passes through the transiently disrupted barrier or endothelial junctions to transfect the target cells, which allows the plasmid DNA to enter the nuclei to produce transgene expression.<sup>18,19</sup> Recent studies have successfully used UMGD to enhance ligament reconstruction<sup>20</sup> and achieve gene transfer across the blood-brain barrier in large animals.<sup>21-24</sup> However, most studies were carried out in small animals, and the clinical relevance of those studies is yet to be determined.<sup>16,18</sup> By using a minimally invasive interventional radiology technique, we delivered the plasmid-carrying therapeutic genes and MBs via a balloon catheter under fluoroscopy guidance, and the therapeutic ultrasound transducer was applied transcutaneously. This novel approach can provide safe and targeted gene therapy to canine livers. We show here that UMGD achieved sustained therapeutic levels of FVIII gene expression for the treatment of hemophilia A, with technology that is feasibly adaptable to clinical applications.

## Methods

### Animal use protocol and canine surgery

All procedures were performed according to the guidelines for animal care for the Seattle Children's Research Institute (SCRI) and the National Institutes of Health. Protocols were approved by the Institutional Animal Care and Use Committees of SCRI, the University of Washington, and Fred Hutchinson Cancer Research Center. Canines were beagles or beagle mixes. The transcutaneous UMGD procedure was described previously.<sup>13</sup> Briefly, the dog was anesthetized, and a balloon catheter was inserted into the jugular vein and placed in the hepatic venous branch to occlude blood flow under fluoroscopy guidance (OEC 9900 Elite Mobil C-Arm X; GE Healthcare). The balloon was placed in the left and middle hepatic vein with the catheter tip located at the orifice of the vein branches. The details of catheter insertion are described in supplemental Methods. The inflated balloon completely obstructed the blood flow in the hepatic vein, which ensured that the MB-plasmid solution was pushed into the hepatic sinusoids under a constant pressure. An MB-plasmid solution (2 mL/kg containing 0.67 mg/kg pHP-hF8-X10, 0.1 mL/kg MBs, 0.2 mL/kg 50% glucose, and phosphate-buffered saline to total weight-based volume) was injected to the occluded hepatic region within 4 minutes, and the injection was timed every 10 seconds to ensure a constant injection rate. The catheter location and the injection parameters were the same for each dog. Transcutaneous therapeutic ultrasound was applied simultaneously to the injected lobe for 8 minutes. The distribution of MBs in the target liver lobe was visualized by a diagnostic ultrasound imaging system (Sonosite).

### Plasmid and MB preparation

The hepatocyte-specific FVIII plasmid construct, pHP-hF8-X10, was made by replacing the B-domain deleted (BDD)-hF8/N6 complementary DNA (cDNA) in the pHP-hF8/N6A plasmid<sup>25</sup> with a BDD hF8 variant (BDD-hF8-X10) cDNA.<sup>26-28</sup> The BDD-hF8-X10 cDNA encodes a human FVIII (hFVIII) variant with 10 amino acid porcine FVIII-like substitutions (I86V, Y105F, A108S, D115E, Q117H, F129L, G132K, H134Q, M147T, and L152P) in the A1 domain of the FVIII heavy chain to increase FVIII gene expression levels.<sup>26-28</sup>

Preparation of RN18 MBs was previously reported<sup>29</sup> and is briefly described in supplemental Methods.

### Analysis of FVIII expression, plasmid copy number, blood chemistry, cytokine levels, and histology

FVIII expression in canine plasma was analyzed by using an hFVIII-specific enzyme-linked immunosorbent assay (ELISA). Plasmid copy numbers in dog liver sections were analyzed by quantitative polymerase chain reaction (qPCR). Details regarding these 2 methods and statistical analysis of the PCR data are provided in supplemental Methods. Whole blood was collected from dogs at multiple time points and was sent to Phoenix Central Laboratory for complete blood counts and chemistry panels (including measurement of aspartate aminotransferase [AST] and alanine aminotransferase [ALT]) to assess liver damage after the procedure. Plasma cytokine levels in treated dog plasma at day 0 (before treatment) and at 1, 3, and 7 days after treatment were evaluated by a dog cytokine 13-plex assay (Eve Technologies). The dogs were euthanized at either 30 days (FLR001) or 60 days (FLR002, FLR004), and whole livers were collected. Liver sections were harvested from both treated and untreated lobes. Hematoxylin and eosin and trichrome stains were used to assess any damage in the liver tissue.

### RNAscope 2.5 High Definition (HD) – Red Assay

At 30 or 60 days after the procedure, the dogs were euthanized, and livers were harvested and sectioned according to an alphanumeric grid. Selected 7- $\mu$ m cryosections were dehydrated in 50%, 70%, or 100% ethanol and stored in 100% ethanol overnight. Hydrogen peroxide (Advanced Cell Diagnostics [ACD]) was added for 10 minutes, and then protease inhibitor IV (ACD) was added for 30 minutes at room temperature. The slides were then subjected to the RNAscope 2.5 HD – Red Assay according to standard protocols from ACD. Additional details are provided in supplemental Methods.

### Ultrasound transducers and systems

The ultrasound system used was previously described<sup>14</sup> and includes a signal-generating amplifier (JJ & A Instruments) controlled by a custom-designed serial interface (Sonic Concepts). The H114H therapeutic ultrasound transducer is a single-element focused transducer with a focal depth of 45 mm. The focal area of this transducer is  $\sim$ 2 mm wide and 83 mm long.

## Results

### Selection of hepatocyte-specific high-expressing hFVIII plasmid

In our previous studies on nonviral gene transfer of FVIII plasmids in tolerized hemophilia A mice, FVIII expression levels fell several-fold initially and then stabilized over time.<sup>30,31</sup> This was because of an initial drop in episomal plasmids before the vectors could be condensed by histones to form nucleosome-like structures and maintained long term in the nucleus.<sup>25</sup> To achieve persistent therapeutic levels of FVIII expression, we selected the pHP-hF8-X10 plasmid<sup>27</sup> driven by a hepatic locus control region and a liver-specific  $\alpha$ 1-antitrypsin promoter for this study. This plasmid contains a truncated FIX first intron to enhance messenger RNA (mRNA) stability, and a BDD-hF8-X10 cDNA encoding an hFVIII variant protein of which 10 residues in the A1 domain were replaced with porcine residues for enhanced secretion<sup>26-28</sup> (Figure 1A). UMGD of this plasmid can achieve even higher

expression levels in mice compared with our previous construct, pHP-hF8/N6.<sup>27</sup> The hFVIII transgene was used in the normal dog experiments to distinguish between transgene expression and endogenous dog FVIII expression.

### Targeting the liver with a minimally invasive transcutaneous UMGD approach

We used a transjugular-venous approach, in which a balloon catheter was inserted into the hepatic vein in the liver. Upon placement, the balloon catheter was inflated, and Visipaque iodinated x-ray contrast agent was injected to map the vasculature of the liver lobe (Figure 1B; supplemental Figure 1, bottom row). MBs were infused through the balloon catheter, and a diagnostic ultrasound was used to assess the orientation of the liver lobe and visualize the distribution of MBs (Figure 1B; supplemental Figure 1, top row). The therapeutic ultrasound transducer (H114H; center frequency, 1.05 MHz) was placed in an optimal location on the abdomen as determined by

fluoroscopy and diagnostic ultrasound, and a mixture of MBs (0.1 mL/kg) and pHP-hF8-X10 plasmid (0.67 mg/kg) in phosphate-buffered saline (2 mL/kg) was injected via the catheter (Figure 1C). Transcutaneous therapeutic ultrasound was applied to enhance gene transfer with an 8-minute pulsed treatment using H114H under 4.6 MPa peak negative pressure, 200  $\mu$ s pulse duration, and 50 Hz pulse repetition frequency (Figure 2A). The H114H transducer created a focal beam that was 83 mm long at the y-axis ( $y = -41$  mm [left],  $-0$  mm [center],  $-42$  mm [right]). The highest relative pressure is at the focus, which is 45 mm in front of the transducer face, representing the location where the majority of transfection will occur (Figure 2B). When applied to the surface of the abdomen, this transducer is optimized to transfect liver lobes at a depth of 30 to 60 mm. We selected the ultrasound parameters that have previously been shown to effectively target hepatocytes.<sup>13</sup> The process of localizing the liver lobe with angiography and diagnostic ultrasound, followed by treatment with the therapeutic ultrasound

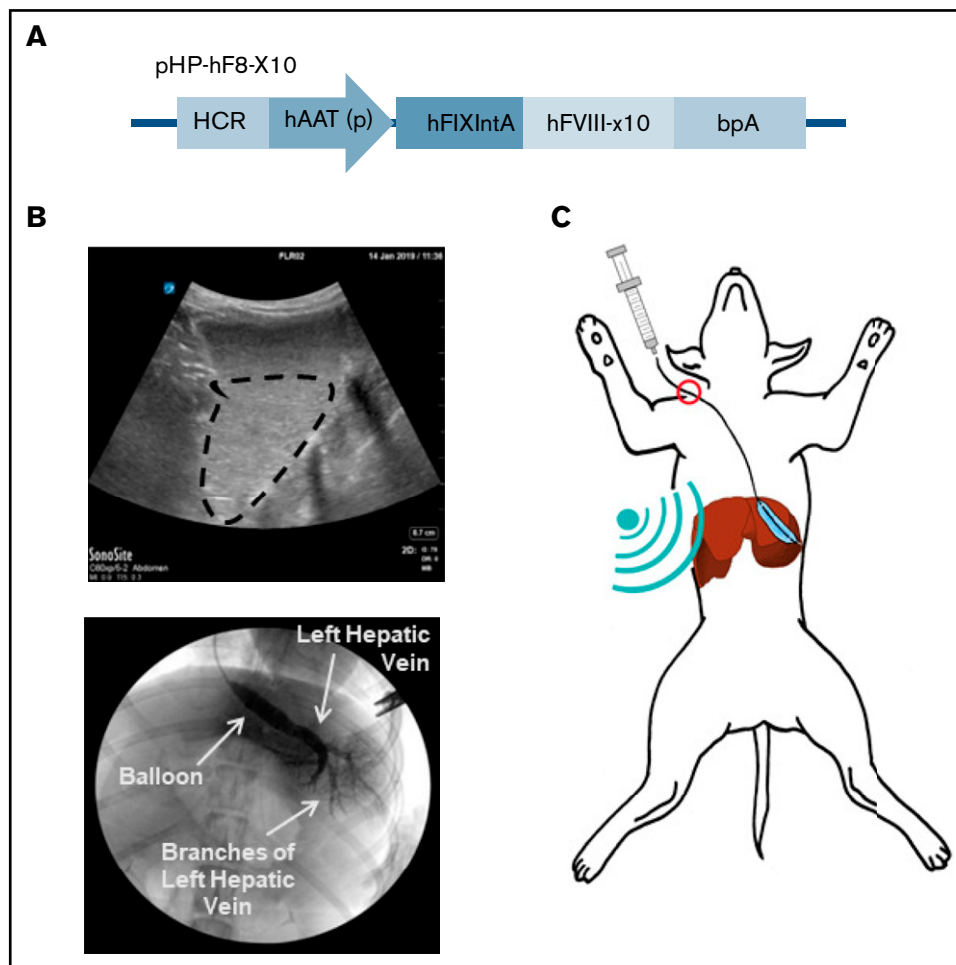


**Figure 1. Liver-targeted transcutaneous UMGD of liver-specific FVIII plasmid into dogs.** (A) The plasmid construct pHP-hF8-X10, which carries an hFVIII variant with 10 residues in the A1 domain of hFVIII replaced with porcine residues (hFVIII-X10), is driven by a liver-specific enhancer-promoter (hepatic locus control region [HCR]-hAAT). (B) A representative diagnostic ultrasound image outlines the dispersion of MBs within the target liver lobe (circled in black, top). Angiography with x-ray contrast (Visipaque) was performed to ensure that the catheter was correctly placed into the hepatic vein and to show widespread agent distribution in the lobe. The bottom of the panel shows placement of the balloon catheter to guide infusion and occlude blood flow from the hepatic vein for LLL treatment. (C) Once the treatment area was identified, pHP-hF8-X10 (0.67 mg/kg) and MBs (0.1 mL/kg) were infused through the catheter as the ultrasound was applied to the surface of the abdomen. bpA, bovine growth hormone polyadenylation signal; hAAT (p), human  $\alpha$ 1-antitrypsin promoter; hFIXIntA, human FIX first intron.

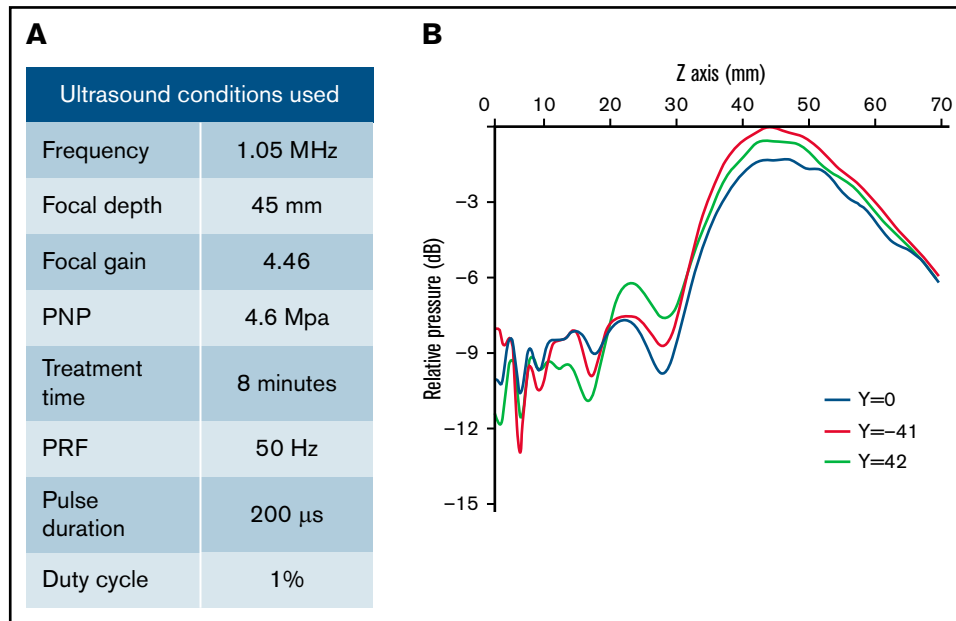


**Figure 2. Therapeutic ultrasound design and parameters used.** (A) Outline of specific ultrasound conditions used in this experiment. (B) Conditions were chosen on the basis of previous experiments that optimized gene transfer in pigs. H114H is a geometrically focused transducer with the highest intensity at 45 mm ( $Z = 45$  mm) from the face of the transducer ( $Z = 0$  mm), shown by a map of relative pressure measured in decibels (dB) using a hydrophone. Measurements were taken at 3 Y locations across the length of the transducer where  $y = -41$  is the left side and  $y = 42$  is the right side relative to the center ( $y = 0$ ) of the transducer.

H114H were repeated for 2 lobes in each dog: the left lateral lobe (LLL) and the right lateral lobe (RLL). No surgical complications were noted in any of the dogs.

### Assessment of blood plasma for hFVIII levels

Four dogs (numbered FLR001 to FLR004) were treated. All dogs were male and ranged between age 1 and 4 years (Figure 3A). After the experiment, blood samples were collected from each dog at multiple time points up to 2 months. The plasma hFVIII antigen levels were examined by using an hFVIII-specific ELISA (Figure 3A-B). All dogs reached therapeutic levels of hFVIII expression within the first week after treatment and 3 of 4 dogs retained expression through the end of the experimental period of 60 days. The level of hFVIII in FLR001 peaked at day 3 with  $\sim 10\%$  of normal plasma hFVIII levels (100%) before dropping to undetectable levels at day 14. The level of hFVIII in FLR002 reached the highest expression level of any of the 4 dogs, with 34% expression on day 3 before dropping to 12%. The level of hFVIII in FLR003 reached 16% on day 2 before declining to 1% by the end of the study. The level of hFVIII expression in FLR004 reached 19% on day 2, which then declined to 7% for the duration of the experiment in a trajectory similar to that of FLR002. Studies have shown that hFVIII levels of  $\sim 10\%$  are considered therapeutic, although levels as low as 1% to 2% still serve to reduce frequency and intensity of bleeds.<sup>10,32</sup> No antibodies to hFVIII were detected in any of the dogs for the duration of the study (data not shown). This is somewhat surprising because it was hypothesized that species-specific anti-hFVIII could be induced in normal dogs. The normal dogs may be tolerant to hFVIII because of the high homology between human and canine FVIII (77% identical and 90% similar amino acid sequence) and the tolerogenic environment in the liver.

### Evaluation of plasmid copy number in treated and untreated lobes

At day 30 for FLR001 and day 60 for FLR002 and FLR004, the treated dogs were euthanized, and livers were harvested and systematically sectioned. FLR003 was released at the end of the experiment because of low levels of FVIII expression. Liver sections were randomly selected (on average,  $\sim 40\%$  of each liver lobe in an evenly distributed pattern) for qPCR analysis to confirm the persistence of plasmids within each liver lobe in treated dogs. Figure 4A (top) shows treated lobes (RLL and LLL) of FLR004, and areas with higher copy numbers are indicated by darker colors. The LLL contains 2 areas of relatively high expression in the top left quadrant and the bottom right quadrant. The highest copy number (445 copies per ng of liver DNA) was observed in this lobe. The RLL contained 1 area of high transfection diagonally down the right side (Figure 4A, bottom). The very small quadrate lobe (QL) was also highly transfected (supplemental Figure 2B). Untreated lobes (lobes that were not exposed to therapeutic ultrasound) had minimal transfection compared with treated lobes (supplemental Figure 3B-D).

There were significant differences in plasmid copy numbers between treated and untreated areas in the target lobes. When the untreated areas of treated lobes were included in the analysis, the average copy number in treated lobes was still significantly higher ( $P < .0001$ ) compared with that in the untreated dog liver control (Figure 4B). FLR001 and FLR002 showed similar patterns of transfection (supplemental Figure 2), although to a lesser degree. FLR001 may have had lower plasmid copy numbers because the plasma level of hFVIII was undetectable at the time of necropsy. FLR002 had higher levels in the caudate lobe (CL), but likely because of a delay in liver harvest, the plasmid copy numbers were not as high as expected based on the hFVIII levels at the time of euthanasia.

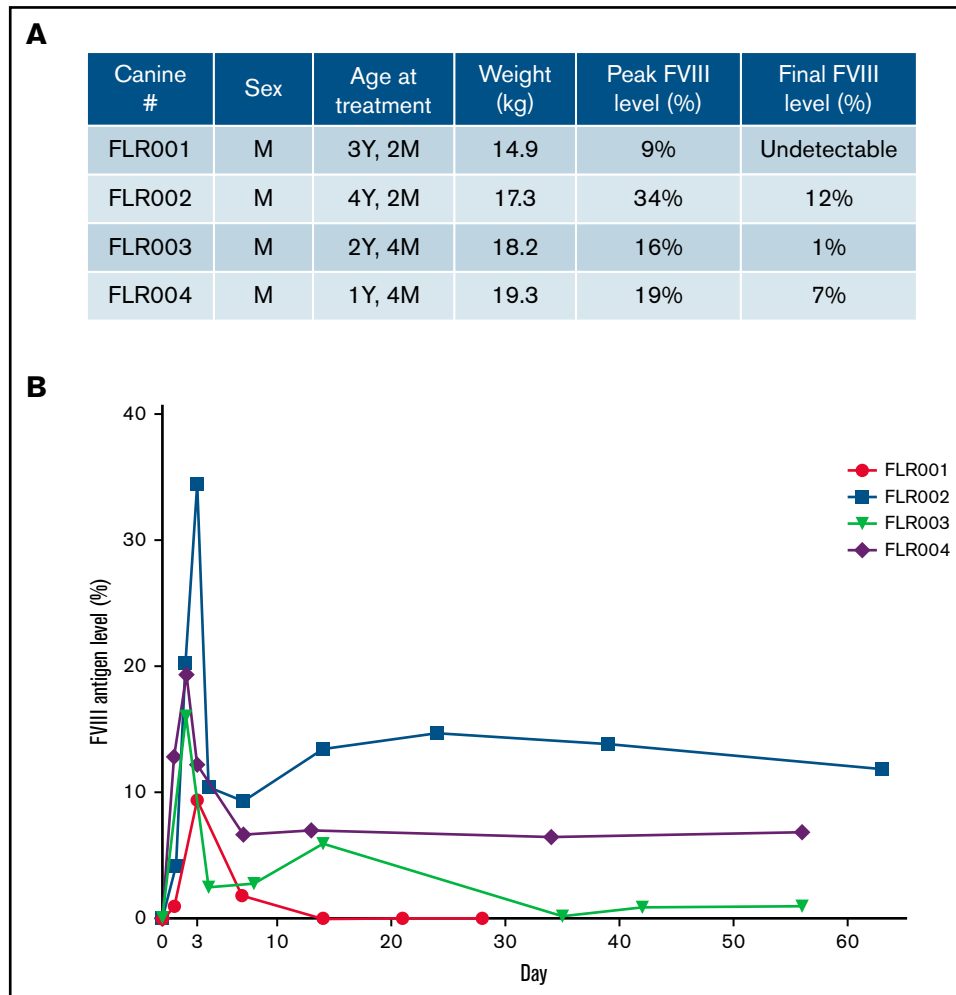


**Figure 3. Therapeutic levels of FVIII expression were detected in canine blood plasma after UMGD.** (A) Male dogs between age 1 and 4 years weighing 14 to 20 kg were used for this study. (B) Four dogs were treated using the transcutaneous UMGD procedure with RN18 MBs under the conditions described in Figure 2 to deliver pHP-hF8-X110. Blood was collected at various time points after the procedure for up to 30 days (FLR001) or 60 days (FLR002, FLR003, and FLR004), and FVIII antigen levels in plasma were evaluated by FVIII-specific enzyme-linked immunosorbent assay (ELISA). Control plasma samples were collected from each individual dog before surgery. Data at each time point is the average of at least 2 ELISAs.

To confirm the presence and specificity of the pHP-hF8-X10 plasmid, a restriction enzyme digest was performed using DNA extracted from a treated lobe (section LLLJ1 from LLL) and an untreated lobe (section LMLG2, from the left medial lobe [LML]) from FLR004 (Figure 4C). Fragments of the expected lengths (50- and 80-bp digested fragments and a 133-bp undigested fragment) were produced in the treated lobe sample and the positive control by using the pHP-hF8-X10 plasmid diluted in canine genomic DNA. No amplified band was detected in the untreated sample from the LML, indicating successful targeting of the plasmid in the target lobes.

### Presence of pHP-hF8-X10 mRNA in treated liver tissue

To ensure that the plasmid present in liver tissue was being actively transcribed, we examined the presence of plasmid-specific mRNA in treated sections. Liver sections were subjected to a specific RNAscope 2.5 HD – Red Assay using 3 different probes. Sections subjected to the RNAscope assay were selected on the basis of

qPCR data. No staining was detected in the treated dog liver tissue with a negative control probe (Figure 5A). A positive control probe that binds a highly expressed control mRNA sequence in dogs validated that the RNA quality of the tissue was preserved (Figure 5B). A custom-designed hFVIII-specific RNAscope probe was used to visualize plasmid-derived mRNA in canine tissue, and a representative image from section D6 of the treated RLL in FLR004 clearly shows the presence of pHP-hF8-X10 mRNA in liver tissue (Figure 5C). These data support FVIII transgene expression (Figure 3) and plasmid DNA copy number results (Figure 4) shown in the previous sections, providing a complete evaluation of transcription and translation of plasmids.

### Blood chemistry levels indicate minimal liver damage

To examine the safety of the transcutaneous UMGD procedure, whole blood biochemistry tests were performed at numerous time points after the surgery. Aside from ALT, AST, and alkaline

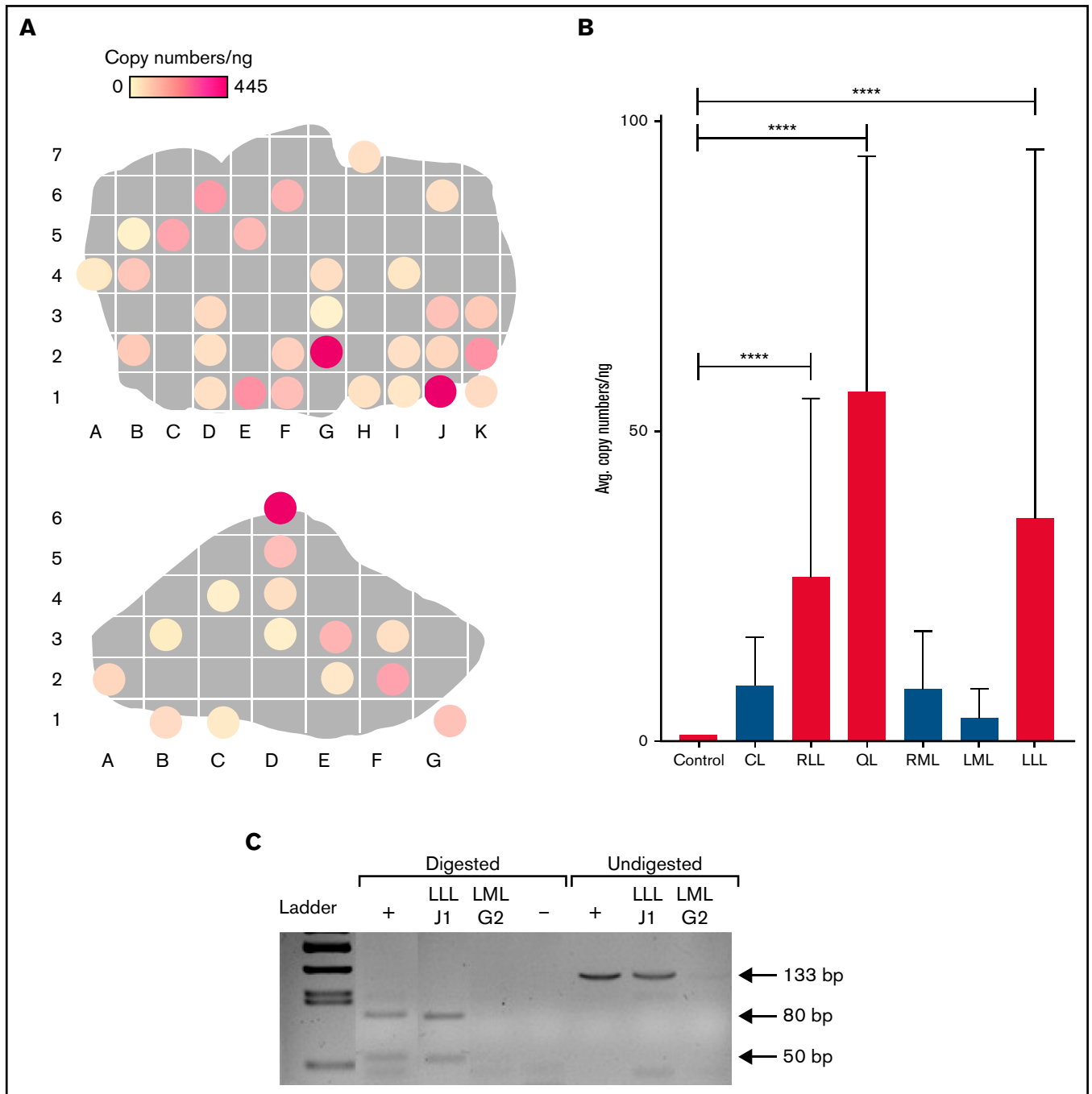


**Figure 4. Distribution of plasmid in FLR004 liver tissue.** (A) Distribution maps show plasmid copy numbers per nanogram in transfected FLR004 liver lobes, which were sectioned according to an alphanumeric grid upon necropsy. The top panel shows the LLL, and the bottom panel shows the RLL. Lighter colors indicate lower copy number, and darker colors indicate higher copy number up to 445 copies per nanogram in the LLL. (B) A summary graph demonstrates comparison of average plasmid copy number per nanogram of genomic DNA among all FLR004 lobes and the untreated canine control. The caudate lobe (CL) (n = 7), RLL (n = 14), quadrate lobe (QL) (n = 4), right medial lobe (RML) (n = 10), left medial lobe (LML) (n = 8), and LLL (n = 29) are shown. Treated lobes are shown in black, and untreated lobes are shown in gray. (C) The PCR fragment amplified from genomic DNA samples isolated from a treated lobe (LLLJ1) and an untreated lobe (LMLG2) were either undigested or digested with *Apa*LI and analyzed by using agarose gel electrophoresis. Digestion of the expected PCR fragment (133 bp) produced 2 fragments ~50 bp and 80 bp long. Plasmid diluted in canine genomic DNA undigested or digested with *Apa*LI was used as the positive control (+), and nuclease-free water digested was used as the negative control. \*\*\*\**P* < .0001.

phosphatase (ALP), parameters examined (creatinine, albumin, bilirubin, and others) were normal at all collection points (Figure 6A; and data not shown). ALT levels were transiently elevated in all dogs,

returning to the normal range within 10 days (Figure 6Ai). Only FLR001 and FLR004 exhibited an AST level outside the normal range, but it returned to normal by day 3 (Figure 6Aii). Only FLR004

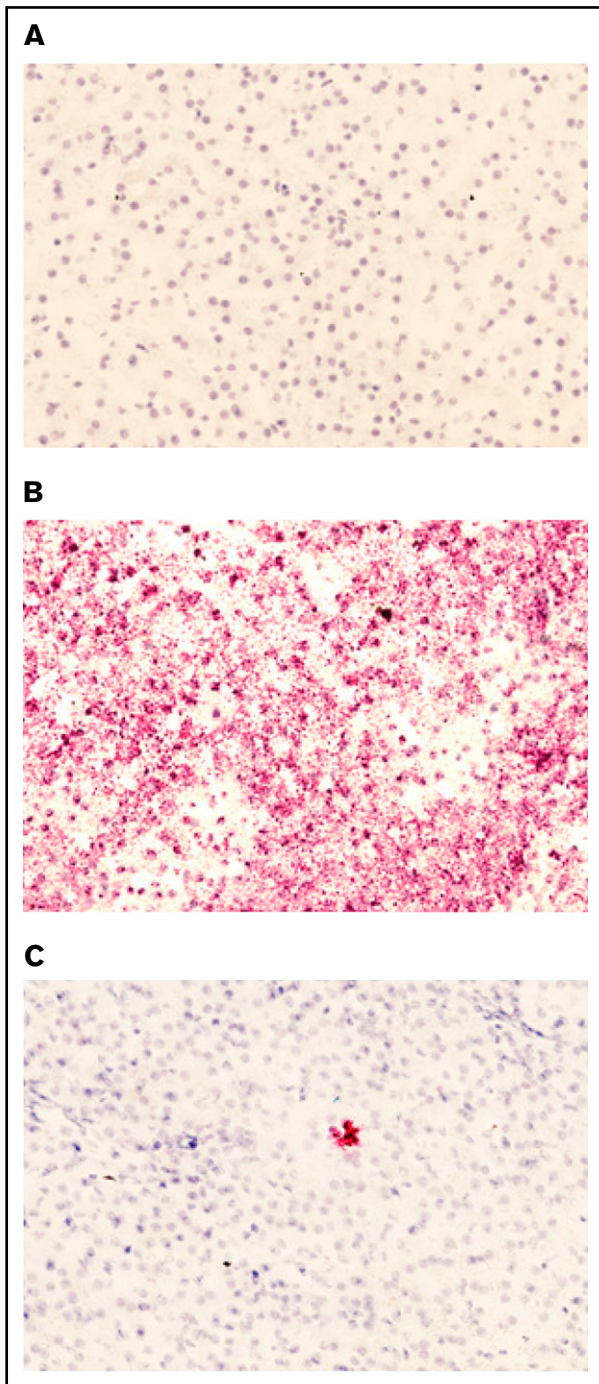


**Figure 5. Presence of pHP-hF8-X10 mRNA in treated canine liver tissue.**

(A) Tissue sections stained with a negative control probe showed no signal, indicating that there was no nonspecific staining. (B) Tissue stained with a positive control probe, which binds a highly expressed canine mRNA sequence, showed widespread staining. (C) Tissue was stained with a probe that specifically binds FVIII mRNA. Red dots indicate the presence of either (B) positive control mRNA or (C) pLP-hF8-X10 mRNA in canine liver tissue collected upon necropsy at 60 days after surgery. Liver was cut into 1-cm squares and frozen in optimal cutting medium, then sectioned at 7 microns and subjected to the RNAscope 2.5 HD – Red Assay. Sections were also stained with hematoxylin to show tissue morphology. Each red dot indicates the presence of 1 copy of pHP-hF8-X10 mRNA in experimental canine tissue. All sections shown are representative selections from the RLL of FLR004, section D6.

had increased ALP levels outside the normal range in the initial few days after treatment; the level returned to the normal range within 2 weeks (Figure 6Av). The slight elevation of transaminase and ALP levels did not require intervention from the veterinary team. In addition, complete blood count data were collected from these dogs before and after treatment at several time points, and there were no significant changes in any of these parameters.

### Histologic analysis of treated canine tissue and blood cytokine analysis

To further examine the impact of our treatment on liver tissue, histologic analysis was performed on tissue sections harvested at 30 days (FLR001, Figure 6Bi) or 60 days (FLR002, Figure 6Bii; FLR004, Figure 6Biii). FLR003 was released from the study at 60 days. There was no macroscopic damage visible on either the liver or the surrounding tissue for FLR001, FLR002, or FLR004. The histology we examined was found to be within the normal range; there was no significant inflammation, fibrosis, or evidence of recent damage or repair. There was mild focal congestion attributed to the necropsy procedure because similar changes were also observed in biopsies from the untreated control liver. Representative sections from the LLL in each dog included a portal triad, lobular hepatocytes, and a central vein.

We examined cytokine levels in the plasma collected from all 4 treated dogs over 7 days after treatment including interferon- $\gamma$  (IFN- $\gamma$ ), interleukin-2 (IL-2), IL-6, IL-8, IL-10, IL-18, Kupffer cell (KC)-like, MCP-1, and tumor necrosis factor- $\alpha$  (TNF- $\alpha$ ) (Figure 7A-I). Despite minor fluctuations of a few cytokines in FLR003 and FLR004, all levels remained in the normal ranges, indicating that the treatment did not induce serious inflammatory responses or toxicities in the treated dogs.

### Discussion

Although many gene therapies for hemophilia A have been investigated, the development of a safe, widely applicable, noninvasive treatment that achieves therapeutic FVIII levels remains elusive. Here, we demonstrate the potential of UMGD as a treatment that fulfills these requirements. Previous studies have optimized transcutaneous UMGD for noninvasiveness and safety.<sup>3,13</sup> A transhepatic venous gene delivery procedure was performed via an interventional radiology method to gain access to the target liver lobe. This procedure is very similar to a wedge hepatic venography, which is a transjugular venous procedure. However, direct wedging of a balloon catheter against the hepatic parenchyma risks hepatic laceration and capsular tear if the injection pressure is too high. Balloon-occluded venography reduces the risks of hepatic injury by spreading the pressure of injection over a large surface area of the hepatic parenchyma. We adjusted catheter placement to liver lobes that can be efficiently targeted transcutaneously in dogs by the therapeutic ultrasound transducer H114H with its focal depth of 45 mm. In this study, no procedural complications were observed, and all dogs rapidly recovered to normal activity levels. Moderate but transient increases in ALT and AST levels were observed, potentially because of MB cavitation that induced minor tissue damage,<sup>2</sup> plasmid induced inflammation, and for other reasons. These dogs were asymptomatic and did not warrant veterinary concern in spite of having elevated transaminase levels. Additional studies will aim to reduce this transient liver injury by optimizing ultrasound parameters and transducers or depleting CpG in plasmids. Most importantly,

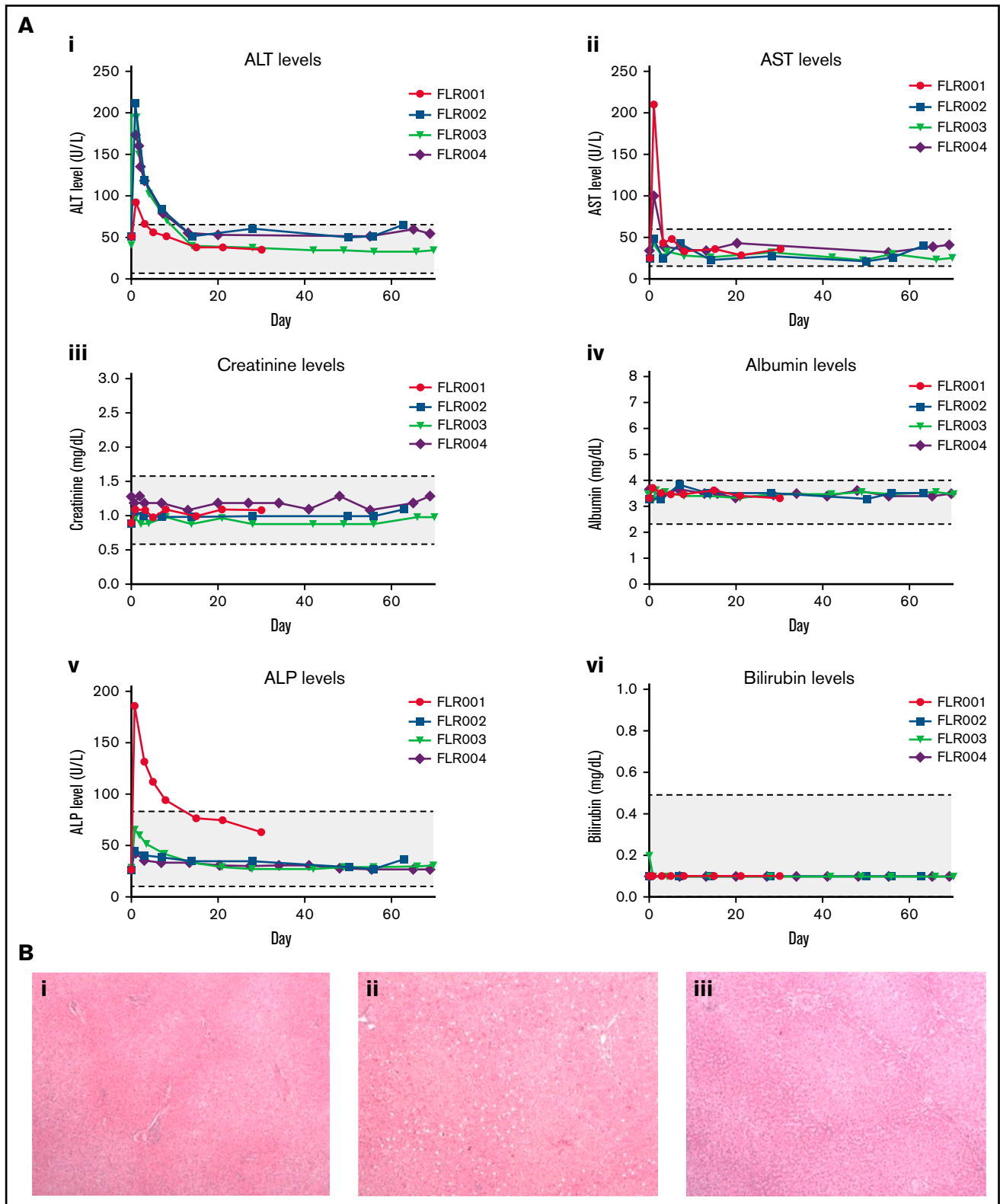


**Figure 6. Examination of potential liver damage after UMGD.** (A) Blood samples were collected from each UMGD-treated dog at multiple time points during week 1 after surgery and then at weekly time points for the length of the study. Several biomarkers were examined to assess liver tissue damage and toxicity: (i) ALT, (ii) AST, (iii) creatinine, (iv) albumin, (v) ALP, (vi) bilirubin, and others (data not shown). Values are plotted with the normal range for dogs indicated in gray. (i) FLR001 was euthanized at 30 days after surgery, and (ii) FLR002 and (iii) FLR004 were euthanized at 60 days after surgery. Liver sections were fixed in 10% formalin, paraffinized, and examined by a pathologist. (B) Slides were stained with hematoxylin and eosin and imaged at 10 $\times$  magnification with representative images shown here. All liver histology is within the normal range, and these sections show treated LLLs from each dog.



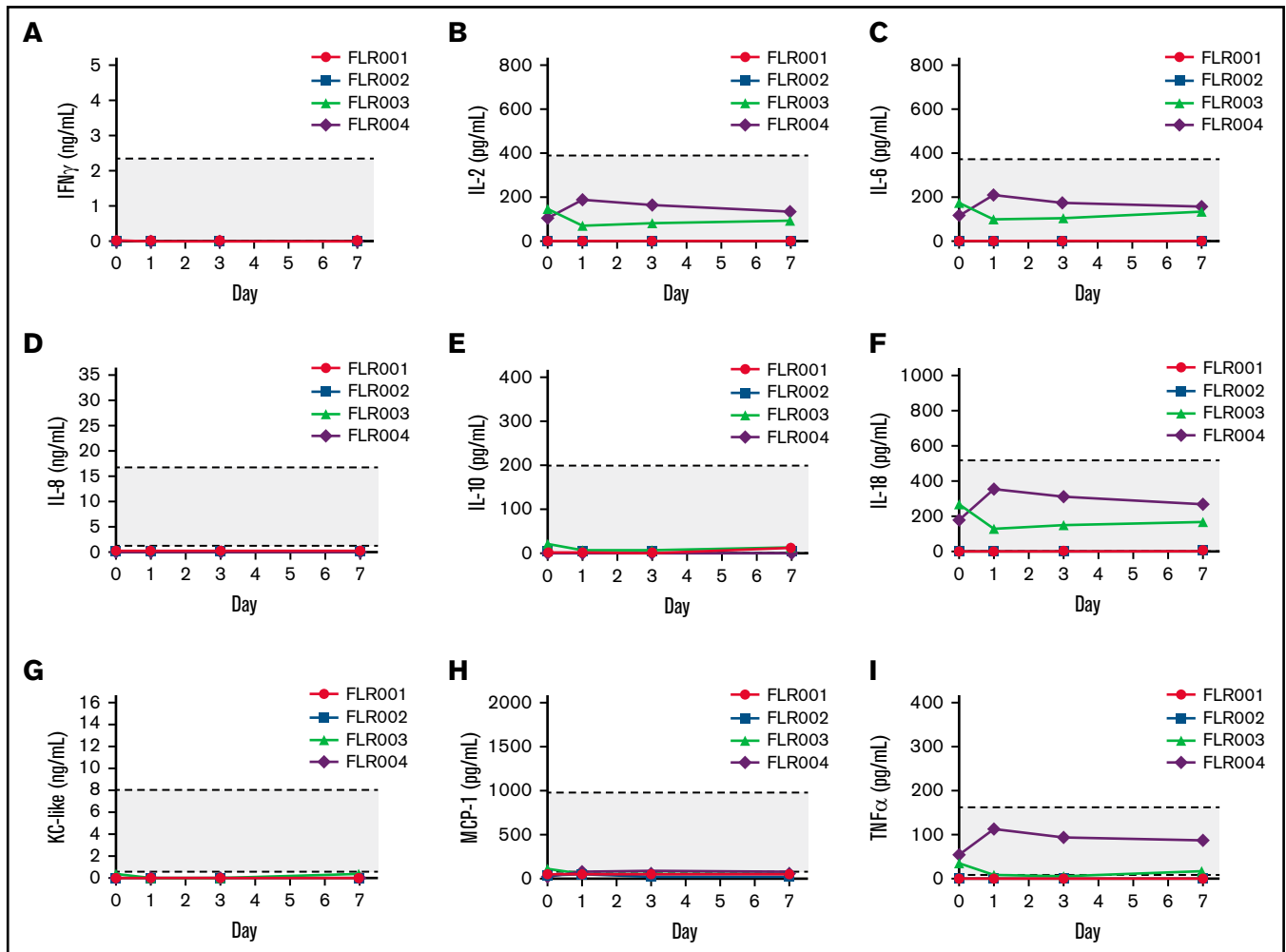


**Figure 7. Examination of plasma cytokine levels after UMGD.** (A) Blood samples were collected from each UMGD-treated dog before treatment (day 0) and at 1, 3, and 7 days after treatment. Several cytokines including (A) IFN- $\gamma$ , (B) IL-2, (C) IL-6, (D) IL-8, (E) IL-10, (F) IL-18, (G) Kupffer cell-like, (H) MCP-1, and (I) TNF- $\alpha$  were examined. Gray area indicates the normal range of each cytokine levels in normal dogs.

these levels returned to normal within 10 days. In addition, complete blood cell counts, along with platelet counts and blood chemistry, showed no significant changes in any of these parameters over time. Histologic examination of the liver tissue at the experimental end point (1-2 months after the procedure) showed no detectable abnormality in the liver tissue. Further analysis of cytokine levels in the treated dog plasma showed that all levels remained in the normal range, indicating that neither UMGD treatment nor plasmid DNA induced significant inflammatory responses or toxicities in the treated dogs. Together these results demonstrate the safety of the transcutaneous UMGD protocol.

In this study, we used our established UMGD procedure to successfully induce therapeutic levels of hFVIII gene expression in normal dogs. Parameters for the severity of hemophilia are well defined: mild hemophilia presents as levels of 5% to 40%, moderate hemophilia presents at 1% to 5%, and severe hemophilia presents in patients with  $\leq 1\%$  of normal FVIII.<sup>10</sup> On the basis of this criteria, 2 of 4 of the treated dogs (FLR002 and FLR004) could be described as having converted severe hemophilia to mild hemophilia after treatment. Our study assessed hFVIII antigen level rather

than functional clotting correction because these normal dogs already had effective clotting ability. However, the hFVIII produced from the same plasmid vector was shown to be fully functional in mouse studies.<sup>33,34</sup> Additional testing in dogs with hemophilia A will demonstrate the functional correction of FVIII deficiency. To put this protocol into the context of treating dogs and patients with hemophilia A, treatment with FVIII or bypassing agent will be used before and after the UMGD procedure to avoid any potential bleeding.

Although expression patterns were similar and appreciable levels of hFVIII expression were induced, hFVIII levels varied among the dogs. These variances are likely inevitable because there were differences in treatment procedures and intracellular processes in different dogs. Similar variability can be seen in viral gene therapy experiments when the same doses of the vectors are administered. Other potential factors could include the gradual improvement of surgical procedures and localization of the plasmids-MBs to the target lobe. Moreover, similar to hydrodynamic delivery,<sup>25,35</sup> plasmids remain predominantly in episomal forms after UMGD. There is a rapid  $\sim$ threefold to fivefold decline of plasmid vector copy numbers in the initial several days before

they reach a plateau. Thus, to achieve therapeutic FVIII expression, more than 10% peak levels probably need to be produced in the initial period. Further improvement of the experimental procedures and development of the next generation of ultrasound transducers are currently ongoing with the goal of achieving higher initial levels of gene expression.

When examining the distribution of plasmid copy numbers in dogs treated with UMGD, the average values in a whole liver lobe were presented. Because of the nature of our gene delivery method and the area of focus of the H114H transducer, the treated lobes contained focal untreated areas which resulted in variable transfection. Despite this, we demonstrated that on average, treated lobes showed significantly higher plasmid copy numbers compared with the control and untreated lobes, indicating significantly enhanced plasmid transfection by UMGD treatment.

Currently, adenoviral-associated vector (AAV)-mediated gene therapies have gained popularity as a promising treatment for hemophilia A.<sup>36-39</sup> Although AAV therapies are progressing toward approval for clinical use, current applications are unavailable to a large portion of patients with hemophilia, including pediatric patients and patients with FVIII inhibitors or preexisting AAV neutralizing antibodies and/or comorbidities.<sup>36,37,40,41</sup> Those who did not have antibodies before gene therapy develop persistently high-titer antibodies to the viral capsid and thus cannot be treated repeatedly.<sup>36,37</sup> Although most studies have not noted genotoxicity after AAV-mediated gene delivery,<sup>42,43</sup> research has shown that AAV vectors have the potential to integrate into the host cell genome,<sup>44</sup> causing clonal expansions and encouraging stricter long-term follow-up.<sup>45,46</sup>

UMGD has emerged as an effective gene transfer approach with great translational potential for treating various diseases.<sup>17,20,47-50</sup> In comparison with viral gene transfer, UMGD transfers plasmid vectors that are relatively easy to prepare and more cost-effective; it also elicits reduced immune responses<sup>14</sup> and prevents random integration into the host genome that can lead to oncogenic events.<sup>51</sup> Common criticisms of UMGD are that gene transfer efficiency is often low, and that the parameters required to perform successful gene delivery can cause tissue damage because of heat accumulation or microvascular damage from MB cavitation. In addition, most studies are performed in vitro or in a small animal model, which leaves questions about their potential relevance to human applications.<sup>16,18</sup> In our study, we showed that UMGD can be optimized to improve gene transfer efficiency in a large animal model and demonstrated promise for translation of this technique to human trials. We also showed that ultrasound transducer design and treatment parameters can be adjusted to minimize tissue damage to asymptomatic levels. Furthermore, we previously demonstrated that with appropriate transgene expression cassettes in the plasmid vectors,

therapeutic levels of transgene expression can be achieved over the lifetime of mice with either hemophilia A<sup>27,30,31</sup> or hemophilia B<sup>52</sup> after nonviral gene transfer. Repeated treatment is feasible and effective in these preclinical models.<sup>52</sup> Long-term gene expression from plasmid DNA has also been demonstrated in many other studies.<sup>53,54</sup> Thus, even if FVIII levels gradually decrease over the long term because of the episomal nature of the plasmid vector, repeated treatment every several years to maintain therapeutic expression could be used to treat a wide population of patients with hemophilia A, and it represents a long-term treatment option for hemophilia A.

Overall, our study establishes the clinical relevance of transcutaneous UMGD. Development of a noninvasive, repeatable, and efficacious UMGD procedure increases the possibility of using a nonviral gene delivery method to treat patients with hemophilia A who are at higher risk of bleeding complications. Our UMGD technology can also be used to target the liver for treating other genetic diseases or can be expanded to include other applications such as gene editing and drug delivery for treating a multitude of conditions.

## Acknowledgments

The authors thank Keaton Weil for her artistic contributions to Figure 1C and Elise Craddock for helping with the experiments.

This work was supported by grants from the National Institutes of Health, National Heart, Lung, and Blood Institute (R01 HL128139 and R01 HL151077) (C.H.M.) and from the National Cancer Institute (R01 CA15704) (R.F.S.).

## Authorship

Contribution: M.A.M. designed and performed experiments, collected and analyzed data, and helped write the manuscript; F.Z. designed and performed surgical procedures and helped write the manuscript; A.N., C.-Y.C., M.P., M.K., and C.C. performed experiments; K.R.L. performed histologic analyses; R.F.S. provided helpful discussions; and C.H.M. developed concepts, directed research, and helped write and edit the manuscript.

Conflict-of-interest disclosure: The authors declare no competing financial interests.

ORCID profiles: F.Z., 0000-0001-5559-8562; A.N., 0000-0002-8975-6730; C.-Y.C., 0000-0001-7199-3271; K.R.L., 0000-0002-3305-0261; M.K., 0000-0001-9377-1354; R.F.S., 0000-0002-9343-4099; C.H.M., 0000-0001-6520-2373.

Correspondence: Carol H. Miao, Seattle Children's Research Institute, 1900 9th Ave, Seattle, WA 98101; e-mail: carol.miao@seattlechildrens.org.

## References

1. Song S, Noble M, Sun S, Chen L, Brayman AA, Miao CH. Efficient microbubble- and ultrasound-mediated plasmid DNA delivery into a specific rat liver lobe via a targeted injection and acoustic exposure using a novel ultrasound system. *Mol Pharm*. 2012;9(8):2187-2196.
2. Noble ML, Kuhr CS, Graves SS, et al. Ultrasound-targeted microbubble destruction-mediated gene delivery into canine livers. *Mol Ther*. 2013; 21(9):1687-1694.
3. Tran DM, Harrang J, Song S, Chen J, Smith BM, Miao CH. Prolonging pulse duration in ultrasound-mediated gene delivery lowers acoustic pressure threshold for efficient gene transfer to cells and small animals. *J Control Release*. 2018;279:345-354.

4. Iorio A, Stonebraker JS, Chambost H, et al. Data and Demographics Committee of the World Federation of Hemophilia. Establishing the prevalence and prevalence at birth of hemophilia in males: a meta-analytic approach using national registries. *Ann Intern Med.* 2019;171(8):540-546.
5. Hotea I, Brinza M, Blag C, et al. Current therapeutic approaches in the management of hemophilia – a consensus view by the Romanian Society of Hematology. *Ann Transl Med.* 2021;9(13):1091.
6. Mancuso ME, Male C, Kenet G, et al. Prophylaxis in children with haemophilia in an evolving treatment landscape. *Haemophilia.* 2021;27(6):889-896.
7. Srivastava A, Santagostino E, Dougall A, et al. WFH Guidelines for the Management of Hemophilia, 3rd edition. *Haemophilia.* 2020;26(suppl 6):1-158.
8. Mannucci PM. Hemophilia therapy: the future has begun. *Haematologica.* 2020;105(3):545-553.
9. Mannucci PM, Tuddenham EG. The hemophilias – from royal genes to gene therapy. *N Engl J Med.* 2001;344(23):1773-1779.
10. Franchini M, Mannucci PM. Hemophilia A in the third millennium. *Blood Rev.* 2013;27(4):179-184.
11. Marchesini E, Morfini M, Valentino L. Recent advances in the treatment of hemophilia: a review. *Biologics.* 2021;15:221-235.
12. Shima M, Nagao A, Taki M, et al. Long-term safety and efficacy of emicizumab for up to 5.8 years and patients' perceptions of symptoms and daily life: a phase 1/2 study in patients with severe haemophilia A. *Haemophilia.* 2021;27(1):81-89.
13. Tran DM, Zhang F, Morrison KP, et al. Transcutaneous ultrasound-mediated nonviral gene delivery to the liver in a porcine model. *Mol Ther Methods Clin Dev.* 2019;14:275-284.
14. Noble-Vranish ML, Song S, Morrison KP, et al. Ultrasound-mediated gene therapy in swine livers using single-element, multi-lensed, high-intensity ultrasound transducers. *Mol Ther Methods Clin Dev.* 2018;10:179-188.
15. Yu J, Chen Z, Yan F. Advances in mechanism studies on ultrasonic gene delivery at cellular level. *Prog Biophys Mol Biol.* 2019;142:1-9.
16. Chowdhury SM, Abou-Elkacem L, Lee T, Dahl J, Lutz AM. Ultrasound and microbubble mediated therapeutic delivery: underlying mechanisms and future outlook. *J Control Release.* 2020;326:75-90.
17. Newman CM, Bettinger T. Gene therapy progress and prospects: ultrasound for gene transfer. *Gene Ther.* 2007;14(6):465-475.
18. Wu J, Li RK. Ultrasound-targeted microbubble destruction in gene therapy: a new tool to cure human diseases. *Genes Dis.* 2016;4(2):64-74.
19. Tomizawa M, Shinozaki F, Motoyoshi Y, Sugiyama T, Yamamoto S, Sueishi M. Sonoporation: gene transfer using ultrasound. *World J Methodol.* 2013;3(4):39-44.
20. Bez M, Kremen TJ, Tawackoli W, et al. Ultrasound-mediated gene delivery enhances tendon allograft integration in mini-pig ligament reconstruction. *Mol Ther.* 2018;26(7):1746-1755.
21. Kamimura HA, Flament J, Valette J, et al. Feedback control of microbubble cavitation for ultrasound-mediated blood-brain barrier disruption in non-human primates under magnetic resonance guidance. *J Cereb Blood Flow Metab.* 2019;39(7):1191-1203.
22. Jones RM, Deng L, Leung K, McMahon D, O'Reilly MA, Hynynen K. Three-dimensional transcranial microbubble imaging for guiding volumetric ultrasound-mediated blood-brain barrier opening. *Theranostics.* 2018;8(11):2909-2926.
23. Fan CH, Lin CY, Liu HL, Yeh CK. Ultrasound targeted CNS gene delivery for Parkinson's disease treatment. *J Control Release.* 2017;261:246-262.
24. Song KH, Harvey BK, Borden MA. State-of-the-art of microbubble-assisted blood-brain barrier disruption. *Theranostics.* 2018;8(16):4393-4408.
25. Miao CH. A novel gene expression system: non-viral gene transfer for hemophilia as model systems. *Adv Genet.* 2005;54:143-177.
26. Cao W, Dong B, Horling F, et al. Minimal essential human factor VIII alterations enhance secretion and gene therapy efficiency. *Mol Ther Methods Clin Dev.* 2020;19:486-495.
27. Song S, Lyle MJ, Noble-Vranish ML, et al. Ultrasound-mediated gene delivery of factor VIII plasmids for hemophilia A gene therapy in mice. *Mol Ther Nucleic Acids.* 2022;27:916-926.
28. Wang X, Fu RY, Li C, et al. Enhancing therapeutic efficacy of in vivo platelet-targeted gene therapy in hemophilia A mice. *Blood Adv.* 2020;4(22):5722-5734.
29. Sun RR, Noble ML, Sun SS, Song S, Miao CH. Development of therapeutic microbubbles for enhancing ultrasound-mediated gene delivery. *J Control Release.* 2014;182:111-120.
30. Liu CL, Ye P, Yen BC, Miao CH. In vivo expansion of regulatory T cells with IL-2/IL-2 mAb complexes prevents anti-factor VIII immune responses in hemophilia A mice treated with factor VIII plasmid-mediated gene therapy. *Mol Ther.* 2011;19(8):1511-1520.
31. Peng B, Ye P, Rawlings DJ, Ochs HD, Miao CH. Anti-CD3 antibodies modulate anti-factor VIII immune responses in hemophilia A mice after factor VIII plasmid-mediated gene therapy. *Blood.* 2009;114(20):4373-4382.
32. Connelly S, Gardner JM, Lyons RM, McClelland A, Kaleko M. Sustained expression of therapeutic levels of human factor VIII in mice. *Blood.* 1996;87(11):4671-4677.
33. Lyle MJ, Harrang J, Tran D, Fu RY, Miao CH. Therapeutic expression of factor VIII following ultrasound-mediated gene delivery of high-expressing FVIII variant plasmids and immunomodulation in hemophilia A mice. The XXVI Congress of the International Society on Thrombosis and Haemostasias, Berlin, Germany, 8-13 July 2017, 1092-PB.
34. Song S, Noble ML, Sun RR, Fan L, Miao CH. Ultrasound and microbubbles mediated factor VIII plasmid gene therapy in hemophilia A mice [abstract]. *Mol Ther.* 2013;21(suppl 1):S41-S42. Abstract 101.

35. Miao CH, Thompson AR, Loeb K, Ye X. Long-term and therapeutic-level hepatic gene expression of human factor IX after naked plasmid transfer in vivo. *Mol Ther*. 2001;3(6):947-957.
36. Perrin GQ, Herzog RW, Markusic DM. Update on clinical gene therapy for hemophilia. *Blood*. 2019;133(5):407-414.
37. Sidonio RF Jr, Pipe SW, Callaghan MU, Valentino LA, Monahan PE, Croteau SE. Discussing investigational AAV gene therapy with hemophilia patients: a guide. *Blood Rev*. 2021;47:100759.
38. Pasi KJ, Rangarajan S, Mitchell N, et al. Multiyear follow-up of AAV5-hFVIII-SQ gene therapy for hemophilia A. *N Engl J Med*. 2020;382(1):29-40.
39. George LA. Hemophilia gene therapy comes of age. *Blood Adv*. 2017;1(26):2591-2599.
40. Pierce GF, Coffin D; Members of the WFH Gene Therapy Round Table Program Committee and Organizing Committee. The 1st WFH Gene Therapy Round Table: Understanding the landscape and challenges of gene therapy for haemophilia around the world. *Haemophilia*. 2019;25(2):189-194.
41. Kruzik A, Fetahagic D, Hartlieb B, et al. Prevalence of anti-adenovirus immune responses in international cohorts of healthy donors. *Mol Ther Methods Clin Dev*. 2019;14:126-133.
42. Chandler RJ, LaFave MC, Varshney GK, et al. Vector design influences hepatic genotoxicity after adeno-associated virus gene therapy. *J Clin Invest*. 2015;125(2):870-880.
43. Niemeyer GP, Herzog RW, Mount J, et al. Long-term correction of inhibitor-prone hemophilia B dogs treated with liver-directed AAV2-mediated factor IX gene therapy. *Blood*. 2009;113(4):797-806.
44. Miao CH, Snyder RO, Schowalter DB, et al. The kinetics of rAAV integration in the liver. *Nat Genet*. 1998;19(1):13-15.
45. Nguyen GN, Everett JK, Kafle S, et al. A long-term study of AAV gene therapy in dogs with hemophilia A identifies clonal expansions of transduced liver cells. *Nat Biotechnol*. 2021;39(1):47-55.
46. Monahan PE, Négrier C, Tarantino M, Valentino LA, Mingozi F. Emerging immunogenicity and genotoxicity considerations of adeno-associated virus vector gene therapy for hemophilia. *J Clin Med*. 2021;10(11):2471.
47. Miao CH, Brayman AA. Ultrasound-mediated gene delivery. In: Yuan X, ed. *Non-Viral Gene Therapy*. Rijeka, Croatia: IntechOpen; 2011:213-242.
48. Price RJ, Fisher DG, Suk JS, Hanes J, Ko HS, Kordower JH. Parkinson's disease gene therapy: will focused ultrasound and nanovectors be the next frontier? *Mov Disord*. 2019;34(9):1279-1282.
49. Chen ZY, Lin Y, Yang F, Jiang L, Ge S. Gene therapy for cardiovascular disease mediated by ultrasound and microbubbles. *Cardiovasc Ultrasound*. 2013;11(1):11.
50. Timbie KF, Mead BP, Price RJ. Drug and gene delivery across the blood-brain barrier with focused ultrasound. *J Control Release*. 2015;219:61-75.
51. Nayak S, Herzog RW. Progress and prospects: immune responses to viral vectors. *Gene Ther*. 2010;17(3):295-304.
52. Ye X, Loeb KR, Stafford DW, Thompson AR, Miao CH. Complete and sustained phenotypic correction of hemophilia B in mice following hepatic gene transfer of a high-expressing human factor IX plasmid. *J Thromb Haemost*. 2003;1(1):103-111.
53. Delalande A, Bouakaz A, Renault G, et al. Ultrasound and microbubble-assisted gene delivery in Achilles tendons: long lasting gene expression and restoration of fibromodulin KO phenotype. *J Control Release*. 2011;156(2):223-230.
54. Sendra L, Herrero MJ, Aliño SF. Translational advances of hydrofection by hydrodynamic injection. *Genes (Basel)*. 2018;9(3):136.